End-Linked Poly(dimethylsiloxane) Elastomers: ^{2}H-Nuclear Magnetic Resonance Investigations of Compression-Induced Segment Anisotropy

Kimberly McLoughlin, J. K. Waldbieser, Claude Cohen,* and T. M. Duncan

School of Chemical Engineering, Cornell University, Olin Hall, Ithaca, New York 14853-5201

Received July 11, 1996; Revised Manuscript Received October 30, 1996[⊗]

ABSTRACT: ^{2}H-NMR spectroscopy is applied to measure strain-induced orientational anisotropy of polymer segments in three environments in poly(dimethylsiloxane) (PDMS) elastomers: elastic chains, pendant chains, and PDMS(d) chains dissolved in the network. The elastomers were prepared with systematically-varied structures and selective deuterium labeling. Network features were inferred from macroscopic measurements using statistical and thermodynamic models. The segment order parameter, S, was found to be proportional to $\lambda^2 - \lambda^{-1}$, where λ is the compression ratio, for the three environments in uniaxially-compressed PDMS networks: elastic chains, pendant chains, and dissolved probe chains. Furthermore, all three environments show the same dependence of the ratio $S/(\lambda^2 - \lambda^{-1})$ on the elastic modulus, in the range 0.089−0.29 MPa. These results agree with the recent theoretical predictions of Brereton and Ries (*Macromolecules* **1996**, *29*, 2644) and thus support the premise that the excluded volume (entropic) interactions between segments subjected to deformation cause anisotropic averaging of the quadrupolar interaction and thus cause a ^{2}H-NMR line splitting.

Introduction

Uniaxial strain induces orientational anisotropy of the polymer segments that constitute elastomeric networks. Induced orientation in mechanically-deformed elastomers has received a lot of attention in recent years, in part due to the molecular level insights provided by ^{2}H-NMR investigations.[1−7] The segment anisotropy is characterized by an order parameter, S, defined as:

$$S = \langle P_2(\cos \psi) \rangle \tag{1}$$

where ψ is the angle between a segment vector and the strain axis and $P_2(\cos \psi)$ is the second Legendre polynomial of cos ψ; the broken brackets represent an average over all segments. Classical elasticity theories[8−10] predict a dependence of S on the deformation ratio, λ ($=L/L_0$), which is corroborated by experiments.[1−5] However, the experimental evidence could be strengthened further by studies of well-characterized network samples.

NMR and optical experiments have also observed orientational anisotropy of probe chains dissolved in uniaxially-strained host networks. The induced alignment of the probe chains has been attributed to a nematic interaction between segments of the probe chains and elastomeric segments of the host network.[4,7] However, the order parameter of the probe chains is approximately equal to the order parameter of the host network,[4,7,11] which is inconsistent with a nematic interaction.[12,13] The relationship between the orientational anisotropy of dissolved chains and the elastic characteristics of host networks has not been investigated, to our knowledge, and is needed to resolve this inconsistency.

We compare here the strain's efficiency at inducing anisotropy, represented by the ratio $S/(\lambda^2 - \lambda^{-1})$ in three elastomeric environments: PDMS(d) networks, PDMS(d) probe chains ($M_n = 16$ kg/mol) dissolved in unlabeled poly(dimethylsiloxane) (PDMS) host networks, and deuterated portions of pendant chains ($M_n = 16$ kg/mol) attached to protonated networks. For each system studied, we correlate $S/(\lambda^2 - \lambda^{-1})$ to network characteristics obtained from swelling measurements. We use networks with systematically-varied elastic and swelling properties prepared by end-linking polymer precursors in the melt state. These networks are well characterized; mechanical and swelling properties, light scattering from swollen samples of similar networks, and ^{2}H-NMR of unconstrained samples have been reported previously.[14−17]

Background

^{2}H-NMR is sensitive to elastomer segment anisotropy through the orientation-dependent quadrupolar interaction. In PDMS(d) the NMR frequency shift caused by the quadrupolar interaction, ν_Q, reflects the time-averaged orientation of a C−^{2}H bond:

$$\nu_Q = \frac{3}{2}\delta_Q \langle P_2(\cos \theta(t)) \rangle \tag{2}$$

where θ is the orientation of a C−^{2}H bond with respect to the external magnetic field, $P_2(\cos \theta(t))$ is the second Legendre polynomial of cos $\theta(t)$, and the broken brackets represent an average over the time of the NMR experiment. δ_Q ($=e^2qQ/h$) is the static quadrupolar coupling, typically 120 kHz for an aliphatic C−^{2}H bond. Equation 2 assumes that the principal axis of the electrostatic field gradient is parallel to the C−^{2}H bond. The distribution of time-averaged C−^{2}H orientations in a sample is the distribution of quadrupolar frequencies and thus is the ^{2}H-NMR spectrum. Because the distribution of C−^{2}H orientations in deuterated elastomers is controlled by the distribution of polymer backbone segment orientations,[9] ^{2}H-NMR spectra are interpreted as experimental measurements of elastomer−segment orientation distributions.[10]

Segments of an undeformed elastomer below its glass transition temperature (T_g) are isotropically-oriented

[⊗] Abstract published in *Advance ACS Abstracts,* February 1, 1997.

S0024-9297(96)01005-4 CCC: $14.00

and fixed in space on the time scale of NMR observation, the inverse of the static quadrupolar coupling ($\sim 10^{-5}$ s). The quadrupolar frequency distribution for static, isotropic segments of an elastomer below T_g is a broad ^{2}H-NMR spectrum whose shape is characteristic of rigid, isotropic solids. The segments of elastomers above T_g move rapidly, which averages the quadrupolar interaction and narrows the ^{2}H-NMR spectrum. In the limit of rapid, isotropic segment motion [$\tau_c \ll 2\pi/\delta_Q$], the quadrupolar interaction is completely averaged, and the ^{2}H-NMR spectrum is reduced to a sharp peak. Unentangled polymer melts satisfy the assumptions of extreme narrowing and exhibit ^{2}H-NMR spectra devoid of quadrupolar broadening.[6]

^{2}H-NMR spectra have been reported for a variety of undeformed elastomers above their glass transition temperatures.[1−7] The spectra have been interpreted as quadrupolar frequency distributions which are incompletely averaged on the time scale of NMR observation, due to constraints imposed by cross-links. Specifically, ^{2}H-NMR spectra of elastomers have been described as the sum of two distinct components contributed by segments of pendant and elastic chains.[12,17,18] Segments of both pendant and elastic chains move rapidly relative to the NMR time scale, as evidenced by the substantially-narrowed ^{2}H-NMR spectrum of the elastomer, compared with the spectrum of the rigid solid. Although segments of undeformed elastomers move rapidly, they do not move isotropically.

Segments of elastic chains are preferentially oriented along elastic-chain end-to-end vectors, which are essentially fixed on the time scale of NMR observation.[19] The elastic-chain end-to-end vectors in undeformed elastomers are oriented isotropically, and the chain dimensions are assumed to have a Gaussian distribution, the same as in un-cross-linked melts.[8,9] The elastic-chain contribution to the ^{2}H-NMR spectrum is predicted by first averaging eq 2 over all orientations compatible with a given, fixed, end-to-end vector and then averaging the resulting expression over the Gaussian distribution of end-to-end vectors.[20] Because elastic-chain segment motions are anisotropic, the motional averaging of the quadrupolar interaction is incomplete and the elastic-chain ^{2}H-NMR component is broader than the spectrum of an un-cross-linked melt.

Unlike the elastic chains, the pendant chains lack fixed end-to-end vectors. Segment motions of unentangled pendant chains are rapid on the NMR time scale, and in undeformed elastomers the motions are isotropic, which completely averages the quadrupolar interaction. Thus, unentangled, pendant-chain contributions to ^{2}H-NMR spectra are narrow, like those of unentangled, un-cross-linked melts.[17] It is important to note that portions of pendant chains constrained by entanglements may not reorient isotropically on the time scale of NMR observation; these constrained portions of pendant chains are expected to contribute to the elastic-chain component of the ^{2}H-NMR spectrum.

Segment motions in an undeformed elastomer average the ^{2}H-NMR spectrum to a single peak. A single peak is observed for an undeformed elastomer because there is an isotropic distribution of end-to-end vectors. Mechanical deformation of elastomers preferentially orients the end-to-end vectors with respect to the strain axis. As a result, motional averaging of the quadrupolar interaction is anisotropic, and the ^{2}H-NMR spectrum splits into two peaks. The ^{2}H-NMR spectral splitting, $\Delta\nu$, induced by uniaxial strain may be predicted by averaging eq 2 over all C−^{2}H bond orientations compatible with end-to-end vectors that are preferentially oriented relative to the strain axis.[1] This averaging leads to an expression for $\Delta\nu$ that depends on the angle between the strain axis and the external magnetic-field direction. For an elastomer strained along an axis parallel to the external magnetic field the splitting is given by:

$$\Delta\nu = \frac{3}{2}\delta_Q\langle P_2(\cos\phi)\rangle\langle P_2(\cos\psi)\rangle \qquad (3)$$

where ϕ is the angle between a C−^{2}H bond and the vector of the segment to which it is attached and ψ is the angle between the segment vector and the strain axis. For an elastomer strained along an axis perpendicular to the external magnetic field, the splitting is one-half that given by eq 3. Because $\langle P_2(\cos\psi)\rangle$ is the segment order parameter, S (see eq 1), eq 3 states that the ^{2}H-NMR spectral splitting, $\Delta\nu$, is directly proportional to the segment order parameter for an elastomer under uniaxial strain.

In this work, we use ^{2}H-NMR to measure segment order parameters for uniaxially-compressed elastomers. Equation 3 is valid for uniaxial tension or compression. Compression is preferable to tension because it accommodates samples with smaller cross sections, which minimizes material requirements for costly deuterium-labeled samples and reduces ^{2}H-NMR spectral broadening owing to field inhomogeneity. In addition, we found it was easy to compress a sample uniformly using parallel plates. In contrast, we found it difficult to apply a uniform uniaxial tension owing to the use of grips which apply additional stresses to the sample.

Ideal rubber-elasticity theories[8,9,21] predict that the order parameter, S, of an elastic-chain segment in a uniaxially-strained elastomer depends on the draw or compression ratio, λ, as:

$$S \propto G_e(\lambda^2 - \lambda^{-1}) \qquad (4)$$

where G_e is the elastic modulus which relates external stress to strain. By combining eqs 1, 3, and 4, one predicts that the NMR splitting in a strained elastomer is proportional to $\lambda^2 - \lambda^{-1}$ as has indeed been observed by ^{2}H-NMR measurements on several deuterated elastomers.[1−5,7] A puzzle arises, however, from the observation that the NMR splitting is proportional to $\lambda^2 - \lambda^{-1}$ for probe solvents[3,5,23−25] and probe polymer chains[4,7,26] dissolved in strained protonated networks.

One solution to this puzzle proposes an energetic nematic coupling between elastic-chain segments and the segment(s) of the dissolved molecules.[6,22,23] Experimental observations of segment anisotropy in probe molecules dissolved in (but not attached to) mechanically-deformed networks have been interpreted as evidence of segment level orientational couplings. The ratio of the segment order parameter of the probe molecules to the segment order parameter of the host network has been termed the orientational coupling constant, ϵ:

$$\epsilon = \frac{S_{probe}}{S_{host}} \qquad (5)$$

Using ^{2}H-NMR, two groups have reported that this ratio is 1 for unentangled short chains with chemical compositions identical with the host networks into which they were dissolved.[4,7] Recently, optical techniques pioneered by Stein[27] have corroborated this result.[11]

Resolution of the puzzle in terms of a nematic-like orientational coupling is unsatisfactory, however, because an orientational coupling constant of 1 indicates that the elastic network chains (which experience both extensional force and nematic orientational coupling) are oriented to the same degree as dissolved chains (which experience only the orientational coupling).[12] An extension of rubber-elasticity theory incorporating nematic interactions[22] predicts indeed that nematic interactions will enhance the orientation of elastic segments and thus lead to an orientational coupling constant less than 1. Recent simulations of induced orientation in probe chains dissolved in stretched, entangled polymer melts concur.[13]

Another solution to the puzzle is that chain segments compete for space, as suggested recently by Ylitalo et al.,[11] which causes an orientational coupling due to entropic interactions. DiMarzio[28] first applied this intermolecular interference (excluded volume) to augment the classical theory of rubber elasticity and explain the empirical Mooney−Rivlin constitutive equation.[29] Several other authors have expanded on DiMarzio's original lattice model.[30−32] DiMarzio's original analysis predicted that the effect of packing entropy should go as $1/M_c$, where M_c is the molecular weight between cross-links. We now know[14,33] that M_c should be instead the molecular weight between *effective* cross-links, which incorporates the effect of trapped entanglements. Since the elastic modulus G_e is proportional to $1/M_c$, the packing entropy effect is also proportional to G_e. A thorough analysis of the effect of this excluded volume interaction on the NMR spectrum for both elastic chains and dissolved chains has very recently been presented by Brereton and Ries.[34] These authors predict that for both network elastic chains and dissolved chains with the same chemical composition as the host network, the ^{2}H-NMR splittings are essentially equal when the molecular weights of dissolved chains and elastic chains are comparable. In addition, the ^{2}H-NMR splittings should be inversely proportional to M_c. We shall compare these predictions with experimental results reported here.

Experimental Procedures

Elastomer Synthesis and Characterization. Poly(dimethylsiloxane) (PDMS) elastomers were produced by end-linking polymer precursors with a tetrafunctional cross-linking agent, using a technique refined by Patel et al.[14] to produce networks with controlled and varied properties. Vinyl-terminated polymer precursors were end-linked via platinum-catalyzed hydrosilation with tetrakis(dimethylsiloxy)silane (A_4) purchased from Huls. Neat difunctional (B_2) and monofunctional (B_1) precursors were combined in carefully controlled ratios with the cross-linking agent. A platinum catalyst, *cis*-dichlorobis(diethylsulfide)platinum II (from Strem Chemical Co.), was dissolved in a minimal amount of toluene and added to the reaction mixture to achieve a concentration of 20 parts of platinum/10^6 parts of siloxane. Networks were cured in polyethylene molds at 35 °C under vacuum; the low curing temperature has been demonstrated to minimize the extent of side reactions.[35] For ^{2}H-NMR measurements of mechanically-deformed elastomers, samples were cut into cubes approximately 0.1 in./side using a razor blade.

B_2 and B_1 precursors were prepared by polymerizing hexamethylcyclotrisiloxane (D_3), using insertion polymerization techniques as detailed previously.[14] Deuterated PDMS elastomers were prepared by end-linking partially-deuterated polymer precursors. Both deuterated and nondeuterated monomers used to produce the deuterium-labeled precursors were synthesized using a reaction sequence adapted from the method described by Beltzung et al.[36]

Table 1. Network Characteristics Derived from End-Linking Reactant Concentrations and from Swelling and Extraction Experiments

sample	M_{n,B_2} (kg/mol)	M_{n,B_1} (kg/mol)	r^a	x^b	W_{sol}	v_{eqm}
Deuterated Networks						
A-1	19		1.7	0.000	0.0061	0.280
A-2	19		1.5	0.000	0.0065	0.277
A-3	19	16	1.7	0.051	0.0172	0.268
A-4	19	16	1.6	0.099	0.0232	0.262
A-5	19	16	1.6	0.173	0.0480	0.242
A-6	19		1.1	0.000	0.102	0.170
A-7	19		1.1	0.000	0.141	0.147
Nondeuterated Networks with Deuterated B_1 Chains						
B-1	16	16	1.7	0.026	0.0122	0.280
B-2	16	16	1.9	0.162	0.0398	0.269
B-3	16	16	1.7	0.081	0.0292	0.268
B-4	16	16	1.8	0.213	0.0796	0.235
B-5	16	16	1.7	0.209	0.0782	0.230
B-6	26	16	1.6	0.167	0.0583	0.197
B-7	16	16	1.7	0.217	0.0961	0.182
B-8	26	16	1.3	0.281	0.1150	0.164
Nondeuterated Networks						
C-1	13		1.7	0.000	0.0070	0.295
C-2	26		1.7	0.000	0.0118	0.254
C-3	32		1.7	0.000	0.0100	0.250
C-4	26	25	1.7	0.114	0.0236	0.229
C-5	26	25	1.7	0.230	0.0596	0.191
C-6	26	29	1.7	0.340	0.0888	0.175

^{a} $r = 4A_4/(B_1 + 2B_2)$. ^{b} $x = B_1/(B_1 + B_2)$.

Three series of end-linked PDMS networks were produced using formulations given in Table 1, where r is the ratio of silane (A) groups to vinyl (B) end groups and x is the mole fraction of monofunctional chains. Networks in series A were produced by end-linking deuterated monofunctional (B_1) and deuterated difunctional (B_2) precursors to yield randomly-deuterated networks. Networks in series B were produced by end-linking deuterated B_1 and nondeuterated B_2 so that only portions of pendant material in these networks were deuterated. Networks in series C were produced using nondeuterated B_2 and nondeuterated B_1; these networks were used for ^{2}H-NMR observations of deuterated probe chains dissolved in nondeuterated networks.

Nondeuterated PDMS networks containing deuterated PDMS(d) probe chains were prepared by placing small amounts (<10 wt %) of deuterated precursor chains on the surfaces of PDMS networks labeled C-1−C-6. The networks were then covered with inverted glass vials and placed in an oven at 60 °C. Chains were assumed to be distributed uniformly throughout the networks when the network surfaces appeared to be completely dry (after approximately 3 days).

The networks were characterized by swelling and extraction in toluene using standard techniques.[37] Soluble fractions, W_{sol}, were determined by comparing network masses before and after toluene extraction of solubles. Equilibrium polymer volume fractions, v_{eqm}, were calculated from mass differences between swollen and dry networks.

^{2}H-NMR of Compressed Elastomers. Elastomer samples were compressed along an axis parallel to the external magnetic field using the device illustrated in Figure 1. The device consists of two Delrin (a product of DuPont) half-cylinders held together by two nylon screws, which are adjusted to compress elastomer samples between the Delrin pieces. Delrin spacers (also shown in Figure 1) of varying thickness were used to ensure that samples were compressed uniformly. At each compression ratio, the sample thickness was measured to the nearest thousandth of an inch using calipers.

^{2}H-NMR data were obtained on a Bruker CXP200 spectrometer operating at 30.72 MHz. Spectra were obtained using a standard 90° pulse of approximate duration 5 ms. Time-domain data were line-broadened by 10 Hz prior to Fourier transformation.

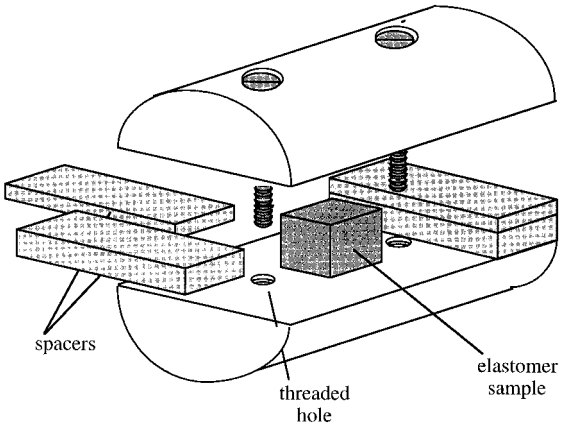

Figure 1. Device used to compress samples for NMR measurements of mechanically-deformed elastomers. The device was oriented such that the compression axis was parallel to the external magnetic field.

Results

Number-averaged molecular weights of polymer precursors obtained using GPC measurements are indicated in Table 1; polydispersities of precursors were found to be less than or equal to 1.1. ^{2}H-NMR spin-counting measurements indicated that 24 wt % of the dimethylsiloxane units in labeled B_2 chains were perdeuterated; 25 wt % of the siloxane units in labeled B_1 chains were perdeuterated.

The amount of soluble material, W_{sol}, and the polymer volume fraction at equilibrium swelling in toluene, v_{eqm}, in the PDMS networks were obtained from extraction and swelling measurements. As demonstrated in Table 1, these characteristics depend on end-linking reactant concentrations given by r, the ratio of silane (A) groups to vinyl (B) end groups, and x, the mole fraction of monofunctional chains. The results shown in Table 1 agree with previous observations that W_{sol} increases and v_{eqm} decreases when x is greater than 0 or when r varies from an optimal value of around 1.7 for producing "model" networks.[14]

The effect of uniaxial compression on the ^{2}H-NMR spectrum for a randomly-deuterated PDMS(d) network is shown in Figure 2. The spectrum observed for the undeformed network ($\lambda = 1$) is a single peak. When the sample is compressed along an axis parallel to the magnetic field, the spectrum splits into a doublet. As strain on the sample increases (indicated by decreasing λ) the spectral splitting, $\Delta\nu$, increases. Increased strain also broadens the spectrum; that is, each component of the doublet is broader than the single peak observed with no strain.

^{2}H-NMR spectra for PDMS(d) probe chains ($M_n = 16$ kg/mol) dissolved in a nondeuterated PDMS network are shown in Figure 3, and spectra for an elastomer in which only monofunctional chains are deuterated are shown in Figure 4. Like the ^{2}H-NMR spectra observed for a randomly-deuterated elastomer, spectra for deuterated monofunctional chains and spectra for chains dissolved in a network split into doublets when the network is compressed; the splitting between the doublet peaks increases with increasing strain. However, ^{2}H-NMR spectra observed for monofunctional chains and for unattached probe chains in undeformed networks are narrower than ^{2}H-NMR spectra observed for the undeformed, randomly-deuterated network. In addition, spectra of monofunctional chains and for unattached probe chains in deformed networks do not broaden appreciably with increasing sample strain; that is, each component of the doublet observed for deuterated probe chains or for deuterated pendant chains has width similar to the single peak observed for the unstrained sample.

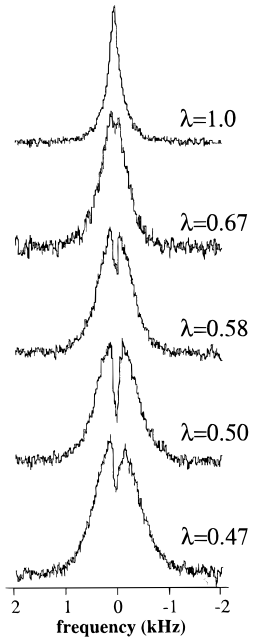

Figure 2. ^{2}H-NMR spectra of compressed PDMS(d) network A-1, prepared by end-linking deuterated B_2 precursors ($\lambda = L/L_0$).

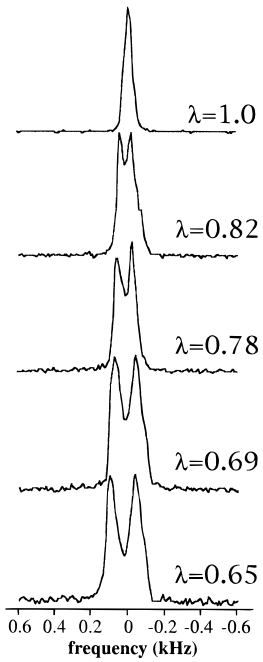

Figure 3. ^{2}H-NMR spectra of PDMS(d) chains dissolved in compressed PDMS network C-2, which was prepared by end-linking nondeuterated B_2 precursors ($\lambda = L/L_0$).

Spectral splittings, $\Delta\nu$, were measured as distances between centers of doublet peaks. The splittings were plotted as a function of $\lambda^2 - \lambda^{-1}$ for each of the networks in this study, as shown in Figures 5, 7, and 8. Error bars in the plots were calculated by assuming an uncertainty of 0.003 in. in the measurements of both the undeformed sample dimension, L_0, and the compressed sample dimension, L.

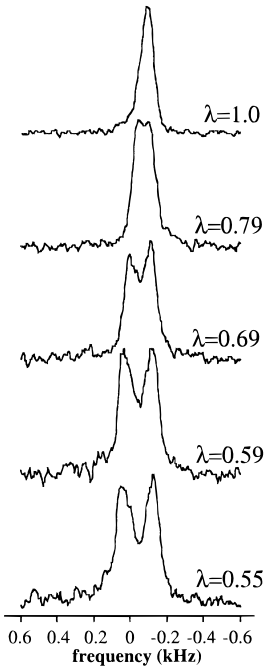

Figure 4. ^{2}H-NMR spectra of compressed PDMS(d) network B-2, prepared by end-linking deuterated B_1 and nondeuterated B_2 precursors ($\lambda = L/L_0$).

Discussion

Characterization of Undeformed Elastomers. Number-average molecular weights between effective cross-links, M_c, of the PDMS networks were obtained from the equilibrium swelling results (Table 1) using the Flory−Rehner model.[38] As demonstrated earlier,[14,39] this model leads to an expression for M_c in terms of v_{eqm}, the polymer volume fraction at equilibrium swelling, χ, the polymer−solvent interaction parameter, and V_1, the molar volume of solvent. Values for M_c obtained using this equation are given in Table 2. Previous studies have demonstrated that values for M_c obtained using this method are inversely proportional to elastic moduli obtained from dynamic mechanical measurements.[14,15,39]

The weight fractions of elastic material, f_{el}, in each of the PDMS networks were determined by applying Macosko and Miller's statistical model for nonlinear polymerization[40−42] as detailed previously.[39] Values for f_{el} determined from end-linking reactant concentrations, r and x, and from the weight fractions of soluble material, W_{sol} (obtained by extraction), are reported in Table 2.

Alternatively, f_{el} for randomly-deuterated networks can be obtained from ^{2}H-NMR transverse-dephasing measurements.[17] The normalized time evolution of the longitudinal magnetization, $M(t)/M(0)$, can be represented as the sum of two components: one contributed by deuterons in segments of elastic chains, $E(t)$, and the other contributed by deuterons in segments of pendant chains, $P(t)$:

$$\frac{M(t)}{M(0)} = f_{el}E(t) + (1 - f_{el})P(t) \qquad (6)$$

The components are distinguished by shape and dephasing rate, due to differences in segment mobility between elastic and pendant chains. Segments of pendant chains reorient isotropically on the NMR time scale, but segments of elastic chains reorient anisotropically, due to constraints at elastic chain ends. As a result, the pendant-chain component, $P(t)$, can be represented by an exponential decay, corresponding to rapid, isotropic motional averaging of the quadrupolar interaction. The elastic-chain component, $E(t)$, is modeled by an expression developed by Cohen-Addad and Dupeyre[19,20] for anisotropic motional averaging of the magnetic interaction which controls transverse dephasing. This simple model for ^{2}H-NMR transverse dephasing (eq 6) contains three adjustable parameters: the weight fraction of elastic chains, f_{el}, and a time constant for each component, t_{el} and t_{pen} for the elastic and pendant components, respectively. Values for f_{el} obtained by fitting the equation to transverse-dephasing data are consistently higher than those obtained using the Macosko−Miller model,[40−42] and the discrepancy increases with increasing f_{el}. We postulated that the difference is because entangled portions of pendant chains may not reorient isotropically on the NMR time scale and thus may contribute to the elastic component of the ^{2}H-NMR dephasing data.[17] Thus, we regard f_{el} values obtained from the Macosko−Miller model as lower bounds for the weight fractions of segments which reorient anisotropically on the NMR time scale due to constraints at chain ends.

Table 2. Network Parameters from Statistical and Thermodynamic Models

sample	G_e (MPa)	M_c (kg/mol)	f_{el}	$p = \Delta\nu/(\lambda^2 - \lambda^{-1})$
		Deuterated Networks		
A-1	0.25	9.6	0.86	−140
A-2	0.25	9.7	0.85	−150
A-3	0.22	11	0.77	−140
A-4	0.22	11	0.73	−130
A-5	0.18	13	0.62	−91
A-6	0.09	28	0.52	−52
A-7	0.06	38	0.46	−32
		Nondeuterated Networks with Deuterated Monofunctional Chains		
B-1	0.25	9.5	0.80	−110
B-2	0.22	11	0.64	−110
B-3	0.22	11	0.70	−120
B-4	0.17	14	0.53	−100
B-5	0.16	15	0.54	−95
B-6	0.11	21	0.60	−60
B-7	0.096	25	0.50	−48
B-8	0.080	30	0.48	−46
		Nondeuterated Networks		
C-1	0.29	8.4	0.85	−150
C-2	0.20	12	0.80	−120
C-3	0.17	14	0.81	−120
C-4	0.16	15	0.72	−79
C-5	0.11	22	0.57	−67
C-6	0.089	27	0.48	−61

Modulus Dependence of Strain-Induced Anisotropy in Compressed PDMS(d) Elastomers. The strain dependence of ^{2}H-NMR spectral splittings observed for a representative set of randomly-deuterated elastomers (series A) compressed along an axis parallel to the external magnetic field is shown in Figure 5. The splittings, $\Delta\nu$, are plotted as a function of $\lambda^2 - \lambda^{-1}$, and they are well-represented by straight lines through the origin (solid and dashed lines in Figure 5), consistent with several previous studies.[1−5,7] The slopes of the best linear fits to $\Delta\nu$ vs $\lambda^2 - \lambda^{-1}$ data are directly proportional to $S/(\lambda^2 - \lambda^{-1})$ and thus measure the efficiency that macroscopic strain orients segments. We will refer to these slopes as strain efficiencies and adopt the definition

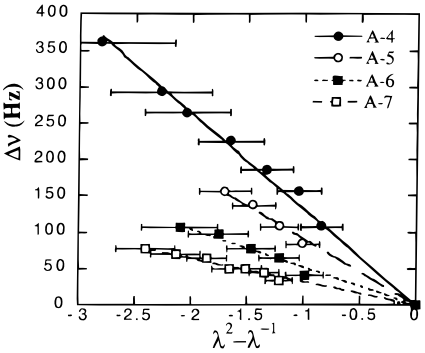

Figure 5. Dependence of ^{2}H-NMR spectral splittings, $\Delta\nu$, on $\lambda^2 - \lambda^{-1}$ for a representative set of PDMS(d) networks prepared by end-linking deuterated B_2 and deuterated B_1 (series A) ($\lambda = L/L_0$).

$$p = \frac{\Delta\nu}{\lambda^2 - \lambda^{-1}} \tag{7}$$

in keeping with earlier studies.[5] The strain efficiencies are reported in Table 2 for all the networks used in this study. The dependence of p on the number-average molecular weight between effective cross-links, M_c, is illustrated by the solid circles in Figure 6 for randomly-deuterated networks. Values of M_c were obtained from equilibrium swelling measurements using the Flory–Rehner model,[38] as detailed above. The data could be represented by a straight line through the origin, indicating that the strain efficiency, p, is inversely proportional to M_c or directly proportional to the elastic modulus, G_e, obtained from mechanical measurements.[14,15]

The earliest theoretical description of the segment order parameter, S, was given by Kuhn and Grun,[9] who calculated the average orientation of the statistical chain segments in perfectly-elastic networks based on the theory of ideal rubber elasticity. Their analysis, combined with the affine assumption,[8] predicts that the segment order parameter is inversely proportional to the average number of segments, N, in an elastic chain:

$$S = \frac{1}{5N}(\lambda^2 - \lambda^{-1}) \tag{8}$$

Because the number of statistical segments, N, is inversely proportional to the elastic modulus, G_e,[8] the order parameter, S, is expected to be directly proportional to G_e, as given in eq 4. The modulus dependence of the segment order parameter was confirmed by Roe and Krigbaum.[21]

Because the ^{2}H-NMR spectral splitting, $\Delta\nu$, is directly proportional to the segment order parameter S (eqs 1 and 3), the results shown in Figure 5 and analogous figures in the literature seem easily interpretable in terms of simple elasticity theories.[8,9,21] As summarized above, these theories show that the segment order parameter is directly proportional to $\lambda^2 - \lambda^{-1}$ at low deformations and the proportionality constant depends linearly on $1/N$ or the elastic modulus. Furthermore, Gronski et al.[43] presented limited data on the ^{2}H-NMR spectral splittings of elastic chains in polybutadiene networks exhibiting the $1/N$ (or $1/M_c$) dependence. Nonetheless, ^{2}H-NMR spectral splittings from probe chains dissolved in deformed elastomers suggest that this interpretation is an oversimplification.

Orientational Coupling between Segments in Compressed PDMS Elastomers. ^{2}H-NMR spectra of PDMS(d) probe chains dissolved in a compressed, nondeuterated PDMS network are shown in Figure 3. Spectral splittings, $\Delta\nu$, increase as sample strain increases, as indicated by decreasing λ. In Figure 7, splittings are plotted as a function of $\lambda^2 - \lambda^{-1}$ for PDMS(d) chains dissolved in a representative set of nondeuterated networks. The data are well-represented by straight lines through the origin (solid and dashed lines.) Thus, like the splittings observed for randomly-deuterated elastomers, the splittings observed for deuterated chains dissolved in strained elastomers are directly proportional to $\lambda^2 - \lambda^{-1}$. This result agrees with several earlier reports.[3,5,7,24]

Slopes of the lines in Figure 7 increase systematically as the elastic modulus of the nondeuterated host networks increases or as the number-average molecular weight between effective cross-links decreases (given in Table 2). The slopes of $\Delta\nu$ vs $\lambda^2 - \lambda^{-1}$ plots, the strain efficiency, obtained for PDMS(d) probes dissolved in networks are reported in Table 2. The polymer volume fraction, ν_{host}, is slightly less than 1 due the presence of the deuterated probe chains in the host networks (Table 3). The correction factor[44] $(\nu_{host})^{-2/3}$ to be applied to S is between 1.0 and 1.1 for our networks and not expected to significantly affect p for probe chains dissolved in the compressed host networks.

The dependence p on the elastic modulus for PDMS(d) probe chains dissolved in unlabeled networks is illustrated by the open squares in Figure 6. Within the scatter of the data for the dissolved probe chains, p is directly proportional to G_e or inversely proportional to

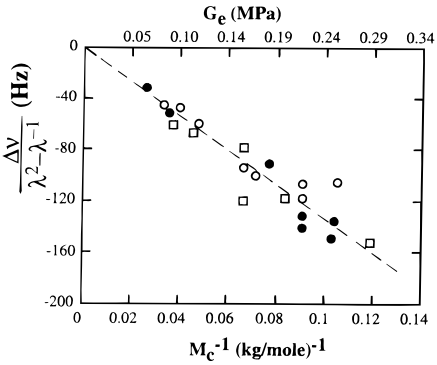

Figure 6. Dependence of $\Delta\nu/(\lambda^2 - \lambda^{-1})$ (Table 2) on the molecular weight between effective cross-links, M_c, and the elastic modulus, G_e, obtained from swelling measurements: (●) data for networks in series A (Figure 5), (○) data for networks in series B (Figure 8), and (□) data for chains dissolved in networks in series C (Figure 7). The dashed line is a guide to the eyes.

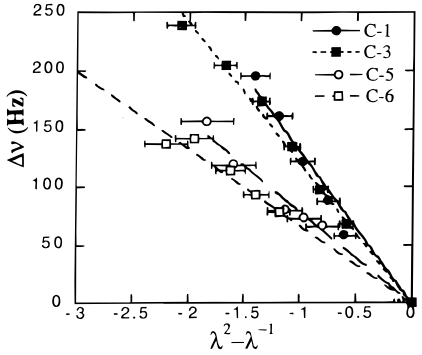

Figure 7. Dependence of ^{2}H-NMR spectral splittings on $\lambda^2 - \lambda^{-1}$ for a representative set of PDMS(d) chains dissolved in networks which were prepared by end-linking nondeuterated B_2 and nondeuterated B_1 (series C) ($\lambda = L/L_0$).

Table 3. Volume Fractions of PDMS Networks Swollen with Probe Chains

host network	ν_{host}	$(\nu_{host})^{-2/3}$
C-1	0.89	1.08
C-2	0.91	1.06
C-3	0.93	1.05
C-4	0.90	1.07
C-5	0.88	1.09
C-6	0.92	1.06

M_c. The modulus dependence of p for these probe chains could be represented by the same straight line through the origin as is the modulus dependence of p observed for randomly-deuterated elastomers. Thus, we infer that the orientational coupling coefficient for PDMS(d) probe chains dissolved in PDMS elastomers is 1 and independent of the elastic modulus of the host network in the range 0.089−0.29 MPa.

Kornfield and co-workers offer an explanation of the identical modulus dependencies of $\Delta\nu$ vs $\lambda^2 - \lambda^{-1}$ data observed for randomly-deuterated networks and for dissolved probe chains.[12] They suggest that central portions of ^{2}H-NMR spectra of elastomers are dominated by contributions from deuterons in pendant chains. Thus, they contend that splittings obtained from peak maxima correspond to order parameters for segments of pendant chains. They argue that using the splitting between peak maxima to infer a single-order parameter for the segments of a network relies on the untested assumption that a single-order parameter describes both pendant- and elastic-chain segment orientations. Their argument that splittings observed by ^{2}H-NMR of strained deuterated elastomers correspond to orientations of pendant-chain segments may be supported by the interpretations that ^{2}H-NMR spectra of undeformed elastomers are linear superpositions of two distinct contributions, corresponding to elastic and pendant chains.[12,17,18] According to these interpretations, pendant chains contribute substantially narrower ^{2}H-NMR peaks than do elastic chains, due to the higher mobility of pendant-chain segments. Thus, pendant-chain contributions may dominate the central portions of ^{2}H-NMR spectra of mechanically-deformed elastomers.

To test this suggestion, we prepared elastomers with deuterium labeling only in pendant chains by end-linking mixtures of deuterated monofunctional chains and nondeuterated difunctional chains. We measured ^{2}H-NMR spectra for these networks (Figure 4) to compare to splittings for compressed, randomly-deuterated networks (Figure 2). The dependence of splittings, $\Delta\nu$, on $\lambda^2 - \lambda^{-1}$ observed for segments of pendant chains attached to compressed networks is shown in Figure 8 for a representative set of networks. The modulus dependence of the slopes of $\Delta\nu$ vs $\lambda^2 - \lambda^{-1}$ data is illustrated by the open circles in Figure 6. Within the error limits of our data, no difference can be detected between splittings for compressed, randomly-deuterated networks and splittings for segments of pendant chains attached to compressed networks. In addition, there is no apparent difference in the modulus dependence of the efficiency of strain-induced segment anisotropy between the randomly-deuterated networks and the networks with deuterated pendant chains.

These observations do not prove or disprove, per se, the suggestion by Kornfield and co-workers[12] because splittings reported for randomly-deuterated networks were obtained from peak maxima which may correspond to pendant-chain contributions to the ^{2}H-NMR spectra.

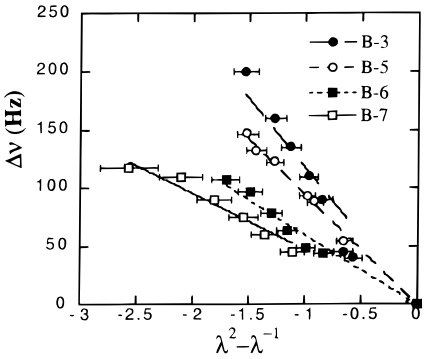

Figure 8. Dependence of ^{2}H-NMR spectral splittings on $\lambda^2 - \lambda^{-1}$ for a representative set of PDMS(d) networks prepared by end-linking nondeuterated B_2 and deuterated B_1 (series B) ($\lambda = L/L_0$).

A conclusive test of their suggestion would require a comparison of ^{2}H-NMR spectra for perfect "model" deuterated networks with no pendant chains to spectra for networks like those in Series B, in which only pendant-chain segments are deuterium-labeled. We believe the end-linking procedure used herein maximizes the fraction of elastic chains, given an appropriate ratio of cross-link molecules to precursor chains.[14] But the procedure cannot produce perfect "model" networks containing only elastic chains; the best "model" network produced still contains a few percent of pendant chains. Nevertheless, we have produced here networks with fractions of elastic chains, f_{el}, which vary, according to the Macosko−Miller statistical model,[40−42] from 0.86 for model networks to 0.46 for imperfect networks. We found previously[17] that ^{2}H-NMR transverse-dephasing measurements consistently predicted slightly higher fractions of elastic chains than did the Macosko−Miller model. Specifically, ^{2}H-NMR measurements predicted 95% elastic chains for the network for which the Macosko−Miller model predicted 86% elastic chains (network A-1).[17] Because this network has only a few percent pendant chains, we expect that contributions from elastic chains dominate the spectral features observed for this network, including the splitting between peaks. This assumption is supported by the observation of very broad spectra obtained for network A-1 (Figure 2). For networks with smaller fractions of elastic chains, f_{el}, we expect that contributions from pendant-chain segments become increasingly significant in determining ^{2}H-NMR spectral splittings. As shown in Table 2, the elastic modulus, G_e, decreases as f_{el} decreases. Thus, if elastic- and pendant-chain segments had significantly different order parameters, we would expect the modulus dependence of the ratio $\Delta\nu/(\lambda^2 - \lambda^{-1})$ (Figure 6) observed for randomly-deuterated networks and the modulus dependence observed for deuterated pendant chains to diverge with varying G_e (corresponding to varying f_{el}). Within the scatter of our data, modulus-dependencies of deuterated pendant chains and randomly-deuterated networks do not diverge as a function of G_e.

We conclude that a single-order parameter describes segment anisotropy in both pendant and elastic chains at any given strain ratio. We further conclude that the orientational coupling constant, ϵ, is 1 for probe chains of the size used here (M_n = 16 kg/mol) dissolved in strained networks of the same chemical composition as the probe chains.

Our results are consistent with the predictions of the recent analytical study of Brereton and Ries[34] based on

an excluded volume interaction rather than an energetic nematic interaction between segments. Their analysis encompasses the more general case of dissolved probe chains with chemical structure different from the host network. They also consider the effect of the molecular weight of the probe chains relative to M_c. In the case of unattached probe molecules with the same chemical structure as the network, their result for the NMR splitting of either elastic-chain segments (denoted by $\Delta\nu_A$) or probe-chain segments (denoted by $\Delta\nu_B$) simplifies to:

$$\frac{\Delta\nu_{A/B}}{\lambda^2 - \lambda^{-1}} = \frac{2}{15\pi^2}\frac{1}{cb^3}\frac{\nu_o}{N_A}\left[\frac{b}{\xi} + O(N_{A/B}^{-1/2})\right] \qquad (9)$$

where b is the average segment length and c is the total segment concentration such that $cb^3 = 1$ in the absence of small-molecule solvents. $N_{A/B}$ represents either the number of segments N_A of an elastic chain or the number of segments N_B of a probe chain. ν_o is an interaction constant and ξ is Edwards screening length.[45] The ratio b/ξ has been estimated to be 4 for PDMS,[34] and the correction term $O(N_{A/B}^{-1/2})$ is negligible here. Thus equal splittings are predicted for both elastic-chain segments and probe-chain segments. In addition, the splittings should depend equivalently on N_A (i.e., M_c). Both predictions are supported by the experimental results reported in Figure 6.

In the above discussion, we have relied on the fact that the concentration of probe chains in series C was small, about 10% of the total concentration. Thus, we assumed c_A/c to be approximately constant, where c_A is the concentration of network segments. However, this raises an issue ignored in the theoretical analysis: what is the role of pendant chains? The model assumes a binary mixture of elastic and probe chains (i.e., $c = c_A + c_B$). If c_A is strictly the concentration of elastic-chain segments (excluding pendant chains), then c_A/c will be proportional to the fraction of elastic chains, f_{el}, which in the networks examined here varies by a factor of 2 (Table 2), according to the statistical model of Miller and Macosko. This variation in f_{el} has been substantiated by ^{2}H-NMR data on unconstrained networks.[17] If we consider our results in Figure 6 for the networks of series A (Table 2), for example, we see that $\Delta\nu/(\lambda^2 - \lambda^{-1})$ depends linearly on $1/M_c$, suggesting that c_A/c is independent of f_{el} and that c_A would include pendant-chain segments in a more complete theoretical analysis incorporating inelastic network segments. If this were the case, $c_A/c = 1$ for series A and B and approximately 0.9 for series C. This difference would be too small to detect given the scatter of our data.

Finally, we observe that the width of each component of the doublet measured for deuterated probe chains is similar to that of the single peak in the unstrained sample (Figure 3), whereas the width of each component of the doublet for the deuterated networks depends on the deformation (Figure 2). This is also predicted by the theory, at least qualitatively.[32,46] Assuming that an elastic chain is compressed under deformation to a new end-to-end length, the number of allowable conformations (and therefore the mobility of the chain) is reduced, which broadens the spectrum. On the other hand, although the segments of a dissolved probe chain are aligned along a preferred orientation as detected by NMR, evidence from neutron scattering[47] indicates that the chain retains the same random quasi-Gaussian conformation as in a melt or an unstrained network. Thus, the allowable conformations of the dissolved chain and its mobility are expected to remain unchanged.

Conclusions

Segment order parameters, S, measured using ^{2}H-NMR for uniaxially-compressed, randomly-deuterated PDMS elastomers depend linearly on $\lambda^2 - \lambda^{-1}$, where λ is the strain ratio. The efficiency with which strain induces segment anisotropy, taken as the ratio $S/(\lambda^2 - \lambda^{-1})$, is directly proportional to the elastic modulus, consistent with previous investigations. In addition, the order parameter depends linearly on $\lambda^2 - \lambda^{-1}$ for PDMS-(d) probe chains dissolved in uniaxially-compressed networks and for deuterated pendant chains attached to uniaxially-compressed networks. For both chains, slopes of linear fits to plots of $\Delta\nu$ vs $\lambda^2 - \lambda^{-1}$ exhibit modulus dependencies identical with those observed for randomly-deuterated elastomers. We conclude that the orientational coupling coefficient, ϵ ($=S_{probe}/S_{host}$), for relatively-short PDMS(d) chains dissolved in PDMS host elastomers is unity, and ϵ is independent of the elastic modulus of the host network in the range 0.089−0.29 MPa. These results and others pertaining to line broadening support Brereton and Ries' recent theoretical analysis[34] attributing the splitting in ^{2}H-NMR spectra to excluded volume interactions between all segments subjected to the deformation. Experiments with probe chains of chemical structure different from that of the host network are needed to further test this theory and shed more light on segmental interactions in elastomers.

Acknowledgment. We thank the National Science Foundation for fellowship support for K.M. We also thank Carol Szeto, who helped synthesize the deuterated polymer samples used in this work. In addition, we are grateful to Reimund Stadler for insightful discussions.

References and Notes

(1) Gronski, W.; Stadler, R.; Jacobi, M. *Macromolecules* **1984**, *17*, 741.
(2) Deloche, B.; Beltzung, M.; Herz, J. *J. Phys. (Paris) Lett.* **1982**, *43*, 763.
(3) Toriumi, H.; Deloche, B.; Herz, J.; Samulski, E. *Macromolecules* **1986**, *19*, 2884.
(4) Sotta, P.; Deloche, B.; Herz, J.; Lapp, A.; Durand, D.; Rabadeux, J.-C. *Macromolecules* **1987**, *20*, 2769.
(5) Dubault, A.; Deloche, B.; Herz, J. *Macromolecules* **1987**, *20*, 2096.
(6) Sotta, P.; Deloche, B. *Macromolecules* **1990**, *23*, 1999.
(7) Jacobi, M.; Abetz, V.; Stadler, R.; Gronski, W. *Polymer* **1996**, *37*, 1669.
(8) Flory, P. J. *Principles of Polymer Chemistry*; Cornell University Press: Ithaca, NY, 1953.
(9) Kuhn, W.; Grun, F. *Kolloid Z.* **1942**, *101*, 248.
(10) Mark, J. E.; Erman, B. *Rubberlike Elasticity: A Molecular Primer*; Wiley-Interscience: New York, 1988.
(11) Ylitalo, C.; Zawada, J.; Fuller, G.; Abetz, V.; Stadler, R. *Polymer* **1992**, *33*, 2949.
(12) Kornfield, J. A.; Chung, G.; Smith, S. *Macromolecules* **1992**, *25*, 4442.
(13) Baljon, A. R. C.; Grest, G. S.; Witten, T. A. *Macromolecules* **1995**, *28*, 1835.
(14) Patel, S.; Malone, S.; Cohen, C.; Gillmor, J.; Colby, R. *Macromolecules* **1992**, *25*, 5241.
(15) Malone, S. P.; Vosburgh, C.; Cohen, C. *Polymer* **1993**, *34*, 5149.
(16) Patel, S. K.; Cohen, C. *Macromolecules* **1992**, *25*, 5252.
(17) McLoughlin, K.; Szeto, C.; Duncan, T. M.; Cohen, C. *Macromolecules* **1996**, *29*, 5475.
(18) Simon, G.; Baumann, K.; Gronski, W. *Macromolecules* **1992**, *25*, 3624.
(19) Cohen-Addad, J. P. *J. Chem. Phys.* **1976**, *64*, 3438.
(20) Cohen-Addad, J. P.; Dupeyre, R. *Polymer* **1983**, *24*, 400.
(21) Roe, R. J.; Krigbaum, W. R. *J. Appl. Phys.* **1964**, *35*, 2215.

(22) Jarry, J.; Monnerie, L. *Macromolecules* **1979**, *12*, 316.
(23) Deloche, B.; Samulski, E. T. *Macromolecules* **1981**, *14*, 575.
(24) Dubault, A.; Deloche, B.; Herz, J. *Polymer* **1984**, *25*, 1405.
(25) Jacobi, M.; Stadler, R.; Gronski, W. *Macromolecules* **1986**, *19*, 2884.
(26) Deloche, B.; Dubault, A.; Herz, J.; Lapp, A. *Europhys. Lett.* **1986**, *1*, 629.
(27) Stein, R. S. *Rubber Chem. Technol.* **1976**, *49*, 458.
(28) DiMarzio, E. A. *J. Chem. Phys.* **1962**, *36*, 1563.
(29) Treloar, L. A. G. *The Physics of Rubber Elasticity*, 2nd ed.; Oxford University Press: London, 1958.
(30) Jackson, J. L.; Shen, M. C.; McQuarrie, D. A. *J. Chem. Phys.* **1966**, *44*, 2388.
(31) Tanaka, T.; Allen, G. *Macromolecules* **1977**, *10*, 426.
(32) Erman, B.; Bahar, I.; Kloczkowski, A.; Mark, J. E. *Macromolecules* **1990**, *23*, 5355.
(33) Ullman, R. *Macromolecules* **1978**, *11*, 987.
(34) Brereton, M. G.; Ries, M. E. *Macromolecules* **1996**, *29*, 2644.
(35) Venkataraman, S. K.; Coyne, L.; Chambon, F.; Gottlieb, M.; Winter, H. H. *Polym. Prepr., Am. Chem. Soc. Div. Polym. Chem.* **1988**, *29*, 571.
(36) Beltzung, M.; Picot, C.; Rempp, P.; Herz, J. *Macromolecules* **1982**, *15*, 1594.
(37) Weiss, P.; Herz, J.; Rempp, P. *Makromol. Chem.* **1970**, *135*, 249.
(38) Flory, P. J.; Rehner, J. *J. Chem. Phys.* **1943**, *11*, 521.
(39) Patel, S. K. Ph.D. Thesis, Cornell University, NY, 1991.
(40) Macosko, C. W.; Miller, D. R. *Macromolecules* **1976**, *9*, 199.
(41) Miller, D. R.; Macosko, C. W. *Macromolecules* **1976**, *9*, 206.
(42) Miller, D. R.; Valles, E. M.; Macosko, C. W. *Polym. Eng. Sci.* **1979**, *19*, 272.
(43) Gronski, W.; Emeis, D.; Brüderlin, A.; Jacobi, M. M.; Stadler, R. *Br. Polym. J.* **1985**, *17*, 103.
(44) Erman, B.; Mark, J. E. *Macromolecules* **1989**, *22*, 480.
(45) Edwards, S. F. *J. Phys. A* **1975**, *8*, 1670.
(46) See eq 5.1 and Figure 3 in Brereton, M. G. *Macromolecules* **1993**, *26*, 1152.
(47) Boué, F.; Farnoux, B.; Bastide, J.; Lapp, A.; Herz, J.; Picot, C. *Europhys. Lett.* **1986**, *1*, 637.

MA961005C